Abstracta

Ano XXVIII - N. 03

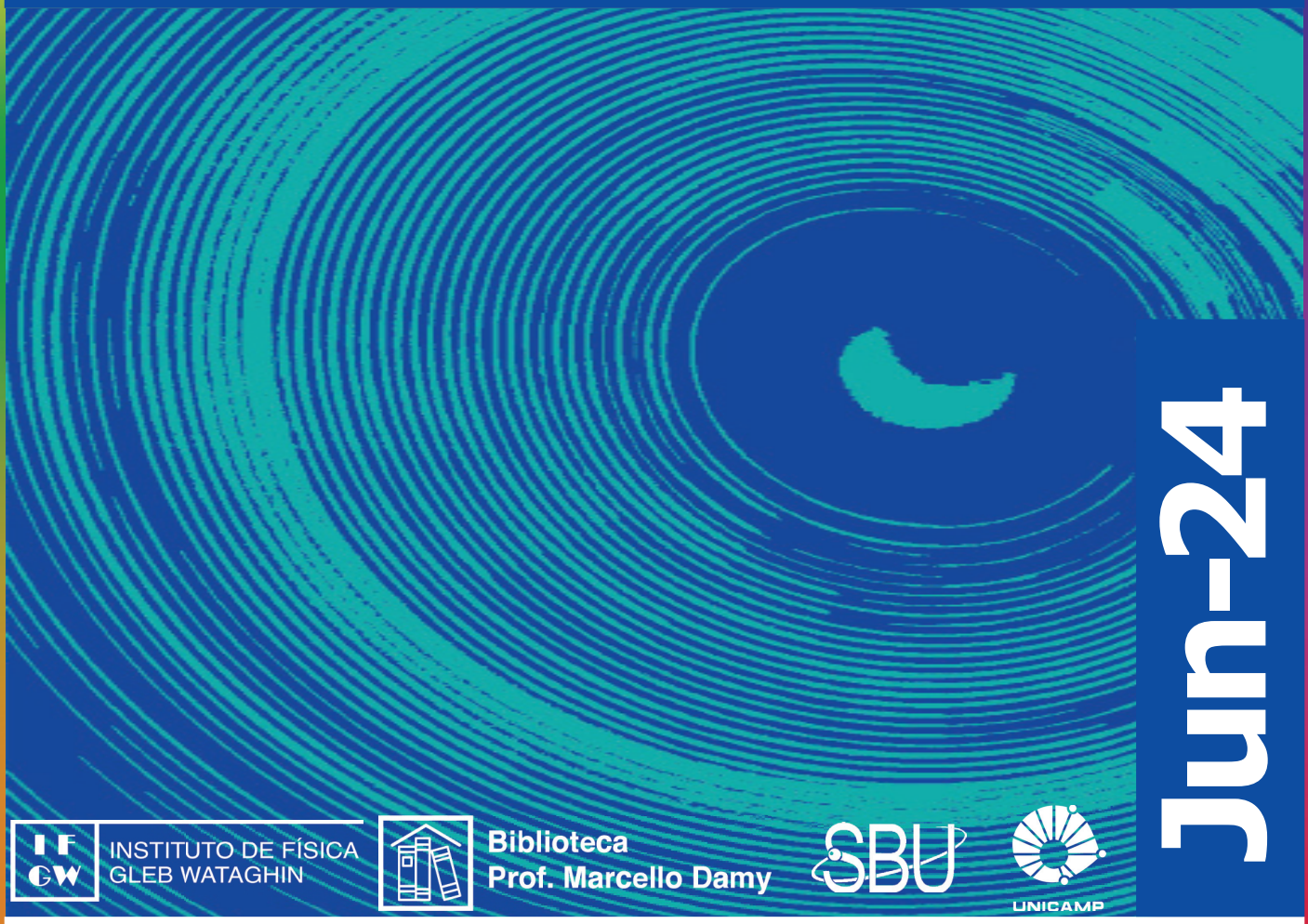

Artigos publicados - P057-2024 à P114-2024

Eventos publicados - P115-2024

Cartas publicadas - Ca001-2024

Defesas de Dissertações do IFGW - D011-2024 à D15-2024

Defesas de Teses do IFGW - T007-2024 à T010-2024

Defesas do PECIM - P003-2024 à P005-2024

Artigos publicados

[P057-2024] "A polarization from vortex rings as the medium response for jet thermalization"

Ribeiro, V. H.*; Chinellato, D. D.*; Lisa, M. A.; Serenone, W. M.; Shen, C.; **Takahashi, J.*; Torrieri, G.***

We performed a systematic study on the formation of vorticity rings as the process for jet thermalization in the medium created in high-energy nuclear collisions. In this work, we expanded our previous analysis to a more realistic framework by considering noncentral events and fluctuations in the initial condition. We simulate the formation and evolution of the flow vortex structure in a relativistic viscous hydrodynamic model and study the sensitivity of the proposed "ring observable" (R-Lambda(t)) that can be measured experimentally through the polarization of Lambda hyperons. We show that this observable is robust with respect to fluctuating initial conditions to capture the jet-induced vortex flow signal and further study its dependence on different model parameters, such as the jet's velocity, position, the fluid's shear viscosity, and the collision centrality. The proposed observable is associated with the formation of vorticity in a quark-gluon plasma, showing that the measurement of particle polarization can be a powerful tool to probe different properties of jet-medium interactions and to understand better the polarization induced by the transverse and longitudinal expansions of the medium.

PHYSICAL REVIEW C 109[1], 014905, 2024. DOI: 10.1103/PhysRevC.109.014905

[P058-2024] "ALICE luminosity determination for Pb-Pb collisions at √sNN=5.02 TeV"

Acharya, S.; Adamová, D.; Adler, A.; **Chinellato, D. D.*; Guardiano, G. G.*; Jahnke, C.*; Takahashi, J.***; et al.
ALICE Collaboration

Luminosity determination within the ALICE experiment is based on the measurement, in van der Meer scans, of the cross sections for visible processes involving one or more detectors (visible cross sections). In 2015 and 2018, the Large Hadron Collider provided Pb-Pb collisions at a centre-of-mass energy per nucleon pair of root s(NN) = 5.02 TeV. Two visible cross sections, associated with particle detection in the Zero Degree Calorimeter (ZDC) and in the V0 detector, were measured in a van der Meer scan. This article describes the experimental set-up and the analysis procedure, and presents the measurement results. The analysis involves a comprehensive study of beam-related effects and an improved fitting procedure, compared to previous ALICE studies, for the extraction of the visible cross section. The resulting uncertainty of both the ZDC-based and the V0-based luminosity measurement for the full sample is 2.5%. The inelastic cross section for hadronic interactions in Pb-Pb collisions at root s(NN) = 5.02 TeV, obtained by efficiency correction of the V0-based visible cross section, was measured to be 7.67 +/- 0.25 b, in agreement with predictions using the Glauber model.

JOURNAL OF INSTRUMENTATION 19[2], P02039, 2024. DOI: 10.1088/1748-0221/19/02/P02039

[P059-2024] "Application of a microfluidic electronic tongue based on impedance spectroscopy for coconut water analysis"

Silva, T. A. da; Juncá, M. A. C.; **Braunger, M. L.*; Riul Jr., A.***; Barbin, D. F.

The food industry has grown with the demands for new products and their authentication, which has not been accompanied by the area of analysis and quality control, thus requiring novel process analytical technologies for food processes. An electronic tongue (e-tongue) is a multisensor system that can characterize complex liquids in a fast and simple way. Here, we tested the efficacy of an impedimetric microfluidic e-tongue setup - comprised by four interdigitated electrodes (IDE) on a printed circuit board (PCB), with four pairs of digits each, being one bare sensor and three coated with different ultrathin nanostructured films with different electrical properties - in the analysis of fresh and industrialized coconut water. Principal Component Analysis (PCA) was applied to observe sample differences, and Partial Least Squares Regression (PLSR) was used to predict sample physicochemical parameters. Linear Discriminant Analysis (LDA) and Partial Least Square - Discriminant Analysis (PLS-DA) were compared to classify samples based on data from the e-tongue device. Results indicate the potential application of the microfluidic e-tongue in the identification of coconut water composition and determination of physicochemical attributes, allowing for classification of samples according to soluble solid content (SSC) and total titratable acidity (TTA) with over 90% accuracy. It was also demonstrated that the microfluidic setup has potential application in the food industry for quality assessment of complex liquid samples.

FOOD RESEARCH INTERNATIONAL 187, 114353, 2024. DOI: 10.1016/j.foodres.2024.114353

[P060-2024] "Bias voltage influence on the a-SiCx:H interlayer deposition using tetramethylsilane: Decorative applications of a-C:H thin films on steel"

Goldbeck, M. C.; Piroli, V.; Weber, J. S.; Boeira, C. D.; Perotti, B. L.; Fukumasu, N. K.; **Alvarez, F.***; Figueroa, C. A.; Michels, A. F.

Hydrogenated amorphous carbon (a-C:H) is a type of coating vastly applied on steel alloys due to its low friction coefficient, high hardness, and chemical inertness. Also, its characteristic brilliant black color like onyx stone is desirable for decorative applications. Despite the beneficial properties conferred to ferrous substrates, the adhesion of a-C:H films is weakened by its residual stress. In order to improve the adhesion of a-C:H films/steel alloy structures, one adopted strategy is the addition of an interlayer. This research investigated the influence of the bias voltage applied on the deposition of hydrogenated amorphous silicon carbide (a-SiCx:H) interlayers, with tetramethylsilane (TMS) as the precursor, to promote adhesion in a-C:H/a-SiCx:H/ferrous alloy structures for decorative applications. The thicker interlayer was achieved at -600 V. Two regimes were proposed to explain this behavior considering ionization rates and resputtering rates and chemical reactions in plasma. The chemical structure in different regions of the a-SiCx:H interlayer was analyzed in detail. An increase in the applied bias voltage leads to oxygen incorporation at the a-C:H/a-SiCx:H interface. Higher bias voltages result in lower silicon content at the a-SiCx:H/steel interface, which is correlated to the -800 V sample's poor adhesion. Finally, we have included a discussion about a new range of loads when a decorative piece is held by the hand where the critical loads for delamination of a-C:H coatings measured here are good enough for decorative applications.

JOURNAL OF VACUUM SCIENCE & TECHNOLOGY A 42[2], 023007, 2024. DOI: 10.1116/6.0003328

[P061-2024] "Can neuromuscular differences manifest by early adolescence in males between predominantly endurance and strength sports?"

Tarrit, B.; Garnier, Y. M.; Birat, A.; **Ruas, C. V.***; Estevam, E.; Rance, M.; Morel, C.; Nottin, S.; Mattiello-Sverzut, A. C.; Nosaka, K.; Blazevich, A. J.; Pinto, R. S.; Ratel, S.

Introduction Although neuromuscular function varies significantly between strength and endurance-trained adult athletes, it has yet to be ascertained whether such differences manifest by early adolescence. The aim of the present study was to compare knee extensor neuromuscular characteristics between adolescent athletes who are representative of strength (wrestling) or endurance (triathlon) sports. Methods Twenty--three triathletes (TRI), 12 wrestlers (WRE) and 12 untrained (CON) male adolescents aged 13 to 15 years participated in the present study. Maximal voluntary isometric contraction (MVIC) knee extensor (KE) torque was measured, and 100-Hz magnetic doublets were delivered to the femoral nerve during and after KE MVIC to quantify the voluntary activation level (%VA). The doublet peak torque (T-100Hz) and normalized vastus lateralis (VL) and rectus femoris (RF) EMG (EMG/M-wave) activities were quantified. VL and RF muscle architecture was also assessed at rest using ultrasound. Results Absolute and relative (to body mass) KE MVIC torques were significantly higher in WRE than TRI and CON ($p < 0.05$), but comparable between TRI and CON. No significant differences were observed between groups for %VA, T-100Hz or either VL or RF muscle thickness. However, VL EMG/M-wave was higher, RF fascicle length longer, and pennation angle smaller in WRE than TRI and CON (all $p < 0.05$). Conclusion The wrestlers were stronger than triathletes and controls, potentially as a result of muscle architectural differences and a greater neural activation. Neuromuscular differences can already be detected by early adolescence in males between predominantly endurance and strength sports, which may result from selection bias and/or physical training.

EUROPEAN JOURNAL OF APPLIED PHYSIOLOGY, 2024. DOI: 10.1007/s00421-024-05480-9

[P062-2024] "Causality violations in simulations of large and small heavy-ion collisions"

Krupczak, R.; Silva, T. N. da; Domingues, T. S.; Luzum, M.; Denicol, G. S.; Gardim, F. G.; Giannini, A. V.; Ferreira, M. N.; Hippert, M.; Noronha, J.; **Chinellato, D. D.*; Takahashi, J.***
ExTrEMe Collaborat

Heavy-ion collisions, such as Pb-Pb or p-Pb, produce extreme conditions in temperature and density that make the hadronic matter transition to a new state, called quark-gluon plasma (QGP). Simulations of heavy-ion collisions provide a way to improve our understanding of the QGP's properties. These simulations are composed of a hybrid description that results in final observables in agreement with accelerators like LHC and RHIC. However, recent works pointed out that these hydrodynamic simulations can display acausal behavior during the evolution in certain regions, indicating a deviation from a faithful representation of the underlying QCD dynamics. To pursue a better understanding of this problem and its consequences, this work simulated two different collision systems, Pb-Pb and p-Pb at root sNN = 5.02 TeV. In this context, our results show that causality violation, even though always present, typically occurs on a small part of the system, quantified by the total energy fraction residing in the acausal region. In addition, the acausal behavior can be reduced with changes in the prehydrodynamic factors and the definition of the bulk-viscous relaxation time. Since these aspects are fairly arbitrary in current simulation models, without solid guidance from the underlying theory, it is reasonable to use the disturbing presence of acausal behavior in current simulations to guide improvements towards more realistic modeling. While this work does not solve the acausality problem, it sheds more light on this issue and also proposes a way to solve this problem in simulations of heavy-ion collisions.

PHYSICAL REVIEW C 109[3], 034908, 2024. DOI: 10.1103/PhysRevC.109.034908

[P063-2024] "Constraining models for the origin of ultra--high-energy cosmic rays with a novel combined analysis of arrival directions, spectrum, and composition data measured at the Pierre Auger Observatory"

Halim, A. A.; Abreu, P.; Aglietta, M.; **Arbeletche, L. B.*; Chinellato, J. A.*; Franco, D. de O.*; Dobrigkeit, C.*; Fauth, A. C.*; Payeras, A. M.***; et al.
Pierre Auger Collaboration

The combined fit of the measured energy spectrum and shower maximum depth distributions of ultra-high-energy cosmic rays is known to constrain the parameters of astrophysical models with homogeneous source distributions. Studies of the distribution of the cosmic-ray arrival directions show a better agreement with models in which a fraction of the flux is non-isotropic and associated with the nearby radio galaxy Centaurus A or with catalogs such as that of starburst galaxies. Here, we present a novel combination of both analyses by a simultaneous fit of arrival directions, energy spectrum, and composition data measured at the Pierre Auger Observatory. The model takes into account a rigidity-dependent magnetic field blurring and an energy-dependent evolution of the catalog contribution shaped by interactions during propagation. We find that a model containing a flux contribution from the starburst galaxy catalog of around 20% at 40 EeV with a magnetic field blurring of around 20 degrees for a rigidity of 10EV provides a fair simultaneous description of all three observables. The starburst galaxy model is favored with a significance of 4.5 sigma (considering experimental systematic effects) compared to a reference model with only homogeneously distributed background sources. By investigating a scenario with Centaurus A as a single source in combination with the homogeneous background, we confirm that this region of the sky provides the dominant contribution to the observed anisotropy signal. Models containing a catalog of jetted active galactic nuclei whose flux scales with the gamma-ray emission are, however, disfavored as they cannot adequately describe the measured arrival directions.

JOURNAL OF COSMOLOGY AND ASTROPARTICLE PHYSICS [1], 022, 2024. DOI: 10.1088/1475-7516/2024/01/022

[P064-2024] "Cosmology from cross-correlation of ACT-DR4 CMB lensing and DES-Y3 cosmic shear"

Shaikh, S.; Harrison, I; van Engelen, A.; **Navarro-Alsina, A.***; et al.
ACT Collaboration; DES Collaboration

Cross-correlation between weak lensing of the Cosmic Microwave Background (CMB) and weak lensing of galaxies offers a way to place robust constraints on cosmological and astrophysical parameters with reduced sensitivity to certain systematic effects affecting individual surveys. We measure the angular cross-power spectrum between the Atacama Cosmology Telescope (ACT) DR4 CMB lensing and the galaxy weak lensing measured by the Dark Energy Survey (DES) Y3 data. Our baseline analysis uses the CMB convergence map derived from ACT-DR4 and Planck data, where most of the contamination due to the thermal Sunyaev Zel'dovich effect is removed, thus avoiding important systematics in the cross--correlation. In our modelling, we consider the nuisance parameters of the photometric uncertainty, multiplicative shear bias and intrinsic alignment of galaxies. The resulting cross--power spectrum has a signal-to-noise ratio = 7.1 and passes a set of null tests. We use it to infer the amplitude of the fluctuations in the matter distribution (S-8 equivalent to sigma(8) (Omega(m)/0.3)(0.5) = 0.782 +/- 0.059) with informative but well-motivated priors on the nuisance parameters. We also investigate the validity of these priors by significantly relaxing them and checking the consistency of the resulting posteriors, finding them consistent, albeit only with relatively weak constraints. This cross-correlation measurement will improve significantly with the new ACT-DR6 lensing map and form a key component of the joint 6x2pt analysis between DES and ACT.

MONTHLY NOTICES OF THE ROYAL ASTRONOMICAL SOCIETY 528[2], 2112-2135, 2024. DOI: 10.1093/mnras/stad3987

[P065-2024] "Cryogenic characterization of Hamamatsu HWB MPPCs for the DUNE photon detection system"

Andreotti, M.; Bertolucci, S.; Branca, A.; **Souza, H. V. de***; et al.

The Deep Underground Neutrino Experiment (DUNE) is a next generation experiment aimed to study neutrino oscillation. Its long-baseline configuration will exploit a Near Detector (ND) and a Far Detector (FD) located at a distance of similar to 1300 km. The FD will consist of four Liquid Argon Time Projection Chamber (LAr TPC) modules. A Photon Detection System (PDS) will be used to detect the scintillation light produced inside the detector after neutrino interactions. The PDS will be based on light collectors coupled to Silicon Photomultipliers (SiPMs). Different photosensor technologies have been proposed and produced in order to identify the best samples to fullfill the experiment requirements. In this paper, we present the procedure and results of a validation campaign for the Hole Wire Bonding (HWB) MPPCs samples produced by Hamamatsu Photonics K.K. (HPK) for the DUNE experiment, referring to them as 'SiPMs'. The protocol for a characterization at cryogenic temperature (77 K) is reported. We present the down-selection criteria and the results obtained during the selection campaign undertaken, along with a study of the main sources of noise of the SiPMs including the investigation of a newly observed phenomenon in this field.

JOURNAL OF INSTRUMENTATION 19[1], T01007, 2023. DOI: 10.1088/1748-0221/19/01/T01007

[P066-2024] "Dark Energy Survey Year 3 results: Simulation-based cosmological inference with wavelet harmonics, scattering transforms, and moments of weak lensing mass maps. Validation on simulations"

Gatti, M.; Jeffrey, N.; Whiteway, L.; **Navarro-Alsina, A.*;** et al.

Beyond-two-point statistics contain additional information on cosmological as well as astrophysical and observational (systematics) parameters. In this methodology paper we provide an end -to -end simulationbased analysis of a set of Gaussian and non-Gaussian weak lensing statistics using detailed mock catalogs of the Dark Energy Survey (DES). We implement: 1) second and third moments; 2) wavelet phase harmonics (WPH); 3) the scattering transform (ST). Our analysis is fully based on simulations, it spans a space of seven nu wCDM cosmological parameters, and it forward models the most relevant sources of systematics of the data (masks, noise variations, clustering of the sources, intrinsic alignments, and shear and redshift calibration). We implement a neural network compression of the summary statistics, and we estimate the parameter posteriors using a likelihood-free-inference approach. We validate the pipeline extensively, and we find that WPH exhibits the strongest performance when combined with second moments, followed by ST, and then by third moments. The combination of all the different statistics further enhances constraints with respect to second moments, up to 25 percent, 15 percent, and 90 percent for S8, omega m, and the figure-of-merit FoMS8;omega m, respectively. We further find that non-Gaussian statistics improve constraints on w and on the amplitude of intrinsic alignment with respect to second moments constraints. The methodological advances presented here are suitable for application to Stage IV surveys from Euclid, Rubin-LSST, and Roman with additional validation on mock catalogs for each survey. In a companion paper we present an application to DES Year 3 data.

PHYSICAL REVIEW D 109[6], 063534, 2024. DOI: 10.1103/PhysRevD.109.063534

[P067-2024] "Demonstrating Agreement between Radio and Fluorescence Measurements of the Depth of Maximum of Extensive Air Showers at the Pierre Auger Observatory"

Halim, A. A.; Abreu, P.; Aglietta, M.; **Arbeletche, L. B.*; Chinellato, J. A.*; Franco, D. de O.*; Dobrigkeit, C.*; Fauth, A. C.*; Payeras, A. M.*; Akim, J. V. R.*;** et al.

We show, for the first time, radio measurements of the depth of shower maximum (Xmax) of air showers induced by cosmic rays that are compared to measurements of the established fluorescence method at the same location. Using measurements at the Pierre Auger Observatory we show full compatibility between our radio and the previously published fluorescence dataset, and between a subset of air showers observed simultaneously with both radio and fluorescence techniques, a measurement setup unique to the Pierre Auger Observatory. Furthermore, we show radio Xmax resolution as a function of energy and demonstrate the ability to make competitive high-resolution Xmax measurements with even a sparse radio array. With this, we show that the radio technique is capable of cosmic-ray mass composition studies, both at Auger and at other experiments.

PHYSICAL REVIEW LETTERS 132[2], 021001, 2024. DOI: 10.1103/PhysRevLett.132.021001

[P068-2024] "Durolon ® polymer as a nuclear track detector: Characterization by chemical etching"

Pires, K. C. C.; Abuchaim, Y.; Kunzel, R.; **Guedes, S.***; Assuncao, M.; Trindade, N. M.; Aquino, R. R. Santos, O. C. B.

This paper presents the properties of alpha particle tracks in a polymer, known as Durolon (R) . The study involves measurements of the time -dependent evolution of etch pit diameters and areal densities for low -energy alpha particles under various etching conditions, including different temperatures and solutions. A time -dependent model was successfully employed to describe the etch pit growth rates. Additionally, optical absorption and Raman spectroscopy techniques were applied to the samples under investigation, complementing the traditional results obtained through optical microscopy. The suitability of Durolon (R) polymer as a nuclear track detector is discussed based on the results obtained from the aforementioned complementary techniques. In summary, this research represents a critical step toward establishing Durolon (R) polymer as a viable nuclear track detector.

RADIATION MEASUREMENTS 175, 107155, 2024. DOI: 10.1016/j.radmeas.2024.107155

[P069-2024] "Engineering large nanoporous networks with size and shape selected by appropriate precursors"

Ceccatto, A.*; Freiberger, E. M.; Waleska-Wellnhofer, N. J.; Jaekel, S.; Mowbray, D. J.; Papp, C.; Steinrück, H. P.; **Siervo, A. de***

Large domains of two-dimensional supramolecular porous nanostructures are interesting for various applications from electronics to biology. Here, we investigate the formation of Cu -coordinated networks on Cu(111) using scanning tunneling microscopy and density functional theory (DFT). We consider two molecules with three pyridyl end groups connected to a central benzene ring by either one or two phenyl groups, namely 1,3,5-tris[4-(pyridin)phenyl]benzene (TPyPB) and 1,3,5-tris[4--(pyridin)-[1,1'-biphenyl]benzene (TPyPPB), respectively. Upon deposition of TPyPB at room temperature, a honeycomb nanostructure forms, which is stabilized by Cu adatoms, as previously seen. Upon deposition at 400 K, the growth dynamics change, and molecules become trapped in the hexagonal pores.

In contrast, deposition of TPyPPB at room temperature leads to vitreous structures, which rearrange at 400 K forming a low -defect and extended ordered honeycomb phase, which is also stabilized only in the presence of Cu adatoms. The DFT calculations for both honeycomb phases show an impressive agreement with the experimental results, considering the size of such structures. After annealing at 420 K, a complex flower-like structure composed of a mix of two- and three -fold coordinated Cu centers emerges. Further annealing to above 420 K leads to another new phase composed of a high molecular density motif, the so-called diamond phase.

CARBON 221, 118945, 2024. DOI: 10.1016/j.carbon.2024.118945

[P070-2024] "Enhanced Elastocaloric Effects in γ-Graphyne"

Kanegae, G. B.*; Pereira Jr., M. L.; **Galvao, D. S.***; Ribeiro Jr., L. A.; **Fonseca, A. F.***

The global emphasis on sustainable technologies has become a paramount concern for nations worldwide. Specifically, numerous sustainable methods are being explored as promising alternatives to the well-established vapor-compression technologies in cooling and heating devices. One such avenue gaining traction within the scientific community is the elastocaloric (eC) effect. This phenomenon holds promise for efficient cooling and heating processes without causing environmental harm. Studies carried out at the nanoscale have demonstrated the efficiency of the eC effect, proving to be comparable to that of state-of-the-art macroscopic systems. In this study, we used classical molecular dynamics simulations to investigate the elastocaloric effect for the recently synthesized gamma--graphyne. Our analysis goes beyond obtaining changes in eC temperature and the coefficient of performance (COP) for two species of gamma-graphyne nanoribbons (armchair and zigzag). We also explore their dependence on various conditions, including whether they are deposited on a substrate or prestrained. Our findings reveal a substantial enhancement in the elastocaloric effect for gamma-graphyne nanoribbons when subjected to prestrain, amplifying it by at least 1 order of magnitude. Under certain conditions, the changes in the eC temperature and the COP of the structures reach expressive values as high as 224 K and 14, respectively. We discuss the implications of these results by examining the shape and behavior of the carbon-carbon bond lengths within the structures.

ACS APPLIED MATERIALS & INTERFACES, 2024. DOI: 10.1021/acsami.4c03302, Early Access Date: MAY 2024

[P071-2024] "Evidence for the Higgs Boson Decay to a Z Boson and a Photon at the LHC"

Aad, G.; Abbott, B.; Abeling, K.; **Chinellato, J. A.***; et al.
ATLAS Collaboration; CMS Collaboration

The first evidence for the Higgs boson decay to a Z boson and a photon is presented, with a statistical significance of 3.4 standard deviations. The result is derived from a combined analysis of the searches performed by the ATLAS and CMS Collaborations with proton -proton collision datasets collected at the CERN Large Hadron Collider (LHC) from 2015 to 2018. These correspond to integrated luminosities of around 140 fb-1 for each experiment, at a center -of -mass energy of 13 TeV. The measured signal yield is 2.2 +/- 0.7 times the standard model prediction, and agrees with the theoretical expectation within 1.9 standard deviations.

PHYSICAL REVIEW LETTERS 132[2], 021803, 2024. DOI: 10.1103/PhysRevLett.132.021803

[P072-2024] "Femtoscopic correlations of identical charged pions and kaons in pp collisions at √s=13 TeV with event--shape selection"

Acharya, S..; Adamova, D.; Rinella, G. A.; **Chinellato, D. D.*; Guardiano, G. G.*; Jahnke, C.*; Liveraro, G. S. S.*; Takahashi, J.***; et al.

Collective behavior has been observed in high-energy heavy-ion collisions for several decades. Collectivity is driven by the high particle multiplicities that are produced in these collisions. At the CERN Large Hadron Collider (LHC), features of collectivity have also been seen in high-multiplicity proton-proton collisions that can attain particle multiplicities comparable to peripheral Pb-Pb collisions. One of the possible signatures of collective behavior is the decrease of femtoscopic radii extracted from pion and kaon pairs emitted from highmultiplicity collisions with increasing pair transverse momentum. This decrease can be described in terms of an approximate transverse mass scaling. In the present work, femtoscopic analyses are carried out by the ALICE Collaboration on charged pion and kaon pairs produced in pp collisions at root s = 13 TeV from the LHC to study possible collectivity in pp collisions. The event--shape analysis method based on transverse sphericity is used to select for spherical versus jetlike events, and the effects of this selection on the femtoscopic radii for both charged pion and kaon pairs are studied. This is the first time this selection method has been applied to charged kaon pairs. An approximate transverse-mass scaling of the radii is found in all multiplicity ranges studied when the difference in the Lorentz boost for pions and kaons is taken into account. This observation does not support the hypothesis of collective expansion of hot and dense matter that should only occur in high-multiplicity events. A possible alternate explanation of the present results is based on a scenario of common emission conditions for pions and kaons in pp collisions for the multiplicity ranges studied.

PHYSICAL REVIEW C 109[2], 024915, 2024. DOI: 10.1103/PhysRevC.109.024915

[P073-2024] "Free Electron-Plasmon Coupling Strength and Near-Field Retrieval through Electron Energy-Dependent Cathodoluminescence Spectroscopy"

Akerboom, E.; Di Giulio, V.; **Schilder, N. J.***; Abajo, F. J. G. de; Polman, A.

Tightly confined optical near fields in plasmonic nanostructures play a pivotal role in important applications ranging from optical sensing to light harvesting. Energetic electrons are ideally suited to probing optical near fields by collecting the resulting cathodoluminescence (CL) light emission. Intriguingly, the CL intensity is determined by the near-field profile along the electron propagation direction, but the retrieval of such field from measurements has remained elusive. Furthermore, the conditions for optimum electron near-field coupling in plasmonic systems are critically dependent on such field and remain experimentally unexplored. In this work, we use electron energy-dependent CL spectroscopy to study the tightly confined dipolar mode in plasmonic gold nanoparticles. By systematically studying gold nanoparticles with diameters in the range of 20-100 nm and electron energies from 4 to 30 keV, we determine how the coupling between swift electrons and the optical near fields depends on the energy of the incoming electron. The strongest coupling is achieved when the electron speed equals the mode phase velocity, meeting the so-called phase-matching condition. In aloof experiments, the measured data are well reproduced by electromagnetic simulations, which explain that larger particles and faster electrons favor a stronger electron near-field coupling. For penetrating electron trajectories, scattering at the particle produces severe corrections of the trajectory that defy existing theories based on the assumption of nonrecoil condition.

Therefore, we develop a first-order recoil correction model that allows us to account for inelastic electron scattering, rendering better agreement with measured data. Finally, we consider the albedo of the particles and find that, to approach unity coupling, a highly confined electric field and very slow electrons are needed, both representing experimental challenges. Our findings explain how to reach unity-order coupling between free electrons and confined excitations, helping us understand fundamental aspects of light-matter interaction at the nanoscale.

ACS NANO 18[21], 13560-13567, 2024. DOI: 10.1021/acsnano.3c12972

[P074-2024] "Hand differences in aiming task: a complementary spatial approach and analysis of dynamic brain networks with EEG"

Fernandes, L. A.; Apolinário-Souza, T.; **Castellano, G.*;** Fortuna, B. C.; Lage, G. M.

Left and right-hand exhibit differences in the execution of movements. Particularly, it has been shown that manual goal--directed aiming is more accurate with the right hand than with the left, which has been explained through the shorter time spent by the right hand in the feedback phase (FB). This explanation makes sense for the temporal aspects of the task; however, there is a lack of explanations for the spatial aspects. The present study hypothesizes that the right hand is more associated with the FB, while the left hand is more strongly associated with the pre-programming phase (PP). In addition, the present study aims to investigate differences between hands in functional brain connectivity (FBC). We hypothesize an increase in FBC of the right hand compared to the left hand. Twenty-two participants performed 20 trials of the goal-directed aiming task with both hands. Overall, the results confirm the study's hypotheses. Although the right hand stopped far from the target at the PP, it exhibited a lower final position error than the left hand. These findings imply that during the FB, the right hand compensates for the higher error observed in the PP, using the visual feedback to approach the target more closely than the left hand. Conversely, the left hand displayed a lower error at the PP than the right. Also, the right hand displayed greater FBC within and between brain hemispheres. This heightened connectivity in the right hand might be associated with inhibitory mechanisms between hemispheres.

BEHAVIOURAL BRAIN RESEARCH 469, 114973, 2024. DOI: 10.1016/j.bbr.2024.114973

[P075-2024] "In Situ PL Tracking of Halide Exchange at 3D/QD Heterojunction Perovskite Solar Cells"

Fonseca, A. F. V.; Scalon, L.; **Vale, B. R. C.***; Guaita, M. G. D.; Bettini, J.; **Brandao, Z. C.*; Zagonel, L. F.*; Padilha, L. A.***; Nogueira, A. F.

Perovskite solar cells (PSCs) show promise for future photovoltaic technology. However, it faces challenges in terms of environmental stability. To address this, researchers have proposed nanomaterials such as perovskite quantum dots (QDs) to passivate the perovskite interfaces and enhance their stability. We explore the halide exchange reaction at the heterojunction between QDs and bulk (3D) perovskites using in situ photoluminescence. By determining the activation energy for the interfacial bromide-to-iodide exchange, we find that it is effective in passivating the 3D surface defects and grain boundaries. When applied in solar cells, QDs have energy level realignment, improving hole extraction and blocking electron transfer, which reduces bimolecular charge carrier recombination, thus increasing efficiency. The interfacial halide composition remains stable under thermal stress, and the QDs' ligand hydrophobicity was found to prevent moisture permeation within the perovskite films. Thus, strategically incorporating QDs enhances photovoltaic performance and has the potential to mitigate moisture and thermal-induced degradation.

ACS ENERGY LETTERS, 2024. DOI: 10.1021/acsenergylett.4c01268 Early Access Date: JUN 2024

[P076-2024] "Jahn-Teller Distortion: A Study of Silver-Bismuth Clusters from First Principles"

Mendoza, E. J. R.; **Silva, E. Z. da***; Ríos, C. L. B.

The recent applications discovered in the use of silver and bismuth nanoalloys, as well as the new environmentally friendly techniques used in their production, have aroused the interest of the scientific community in this study. In this study, we used ab initio density functional theory (DFT) implemented in the Quantum Espresso software to study the structural and electronic properties of silver icosahedral clusters with a bismuth atom by maintaining a similar percentage of bismuth in the existing nanoparticles (similar to 6%). The results indicate a decrease in the magnetization of the cluster with bismuth both in the lateral and central positions, going from 5 [mu B] in the silver cluster to 3 [mu B], and also to a distortion of the structure that leads to a doubling of energy levels, associated with a Jahn-Teller effect, when the bismuth atom was positioned in the lateral position, bringing the structure to a state of lower energy, which agrees with the experimental results.

BRAZILIAN JOURNAL OF PHYSICS 54[4], 115, 2024. DOI: 10.1007/s13538-024-01474-2

[P077-2024] "Luminosity determination using Z boson production at the CMS experiment"

Hayrapetyan, A.; Tumasyan, A.; Adam, W.; **Chinellato, J. A.***; et al.
CMS Collaboration

The measurement of Z boson production is presented as a method to determine the integrated luminosity of CMS data sets. The analysis uses proton-proton collision data, recorded by the CMS experiment at the CERN LHC in 2017 at a center-of-mass energy of 13 TeV. Events with Z bosons decaying into a pair ofmuons are selected. The total number of Z bosons produced in a fiducial volume is determined, together with the identification efficiencies and correlations from the same data set, in small intervals of 20 pb(-1) of integrated luminosity, thus facilitating the efficiency and rate measurement as a function of time and instantaneous luminosity. Using the ratio of the efficiency-corrected numbers of Z bosons, the precisely measured integrated luminosity of one data set is used to determine the luminosity of another. For the first time, a full quantitative uncertainty analysis of the use of Z bosons for the integrated luminosity measurement is performed. The uncertainty in the extrapolation between two data sets, recorded in 2017 at low and high instantaneous luminosity, is less than 0.5%. We show that the Z boson rate measurement constitutes a precise method, complementary to traditional methods, with the potential to improve the measurement of the integrated luminosity.

EUROPEAN PHYSICAL JOURNAL C 84[1], 26, 2024. DOI: 10.1140/epjc/s10052-023-12268-2

[P078-2024] "Magnetic structure and component-separated transitions of HoNiSi3"

Tartaglia, R.*; Arantes, F. R.; **Galdino, C. W.***; Kaneko, U. F.; Avila, M. A.; **Granado, E.***; Vildosola, V.; Nunez, M.; Cornaglia, P. S.; García, D. J.

HoNiSi3 is an intermetallic compound characterized by two successive antiferromagnetic transitions at T-N1 = 6.3K and T-N2 = 10.4K. Here, its zero-field microscopic magnetic structure is inferred from resonant x-ray magnetic diffraction experiments on a single crystalline sample that complement previous bulk magnetic susceptibility data. For T < T-N2, the primitive magnetic unit cell matches the chemical cell. The magnetic structure features ferromagnetic ac planes stacked in an antiferromagnetic up arrow down arrow up arrow down arrow pattern. For T-N1 < T < T-N2, the ordered magnetic moment points along <(a)over right arrow>, and for T < T-N1 a component along <(c)over right arrow> also orders. A symmetry analysis indicates that the magnetic structure for T < T-N1 is not compatible with the presumed orthorhombic Cmmm space group of the chemical structure, and therefore a slight lattice distortion is implied. Mean-field calculations using a simplified magnetic Hamiltonian, including a reduced set of three independent exchange coupling parameters determined by density functional theory calculations and two crystal electric field terms taken as free-fitting parameters, are able to reproduce the main experimental observations. An alternative approach using a more complete model including seven exchange coupling and nine crystal electric field terms is also explored, where the search of the ground state magnetic structure compatible with the available anisotropic magnetic susceptibility and magnetization data is carried out with the help of an unsupervised machine learning algorithm. The possible magnetic configurations are grouped into five clusters, and the cluster that yields the best comparison with the experimental macroscopic data contains the parameters previously found with the simplified model and also predicts the correct ground-state magnetic structure.

PHYSICAL REVIEW B 109[14], 144402, 2024. DOI: 10.1103/PhysRevB.109.144402

[P079-2024] "Martensitic and room-temperature magnetocaloric properties of Mn-rich Mn-Ni-Sn Heusler alloys: Experiment and theory"

Sharma, J.; **Coelho, A. A.***; Suresh, K. G.; Alam, A.

Here, we study the effect of external pressure on martensitic transition, magnetic, and magnetocaloric properties of Mn--rich Mn50Ni41-xSn9+x (x = 0 and 2) Heusler alloys by using a combined experimental and first principles simulation. The x = 0 alloy exhibits martensitic transition around room temperature (RT), which increases appreciably under external pressure for both the alloys. External pressure and magnetic field show opposite effects on martensitic transition (TM). The x = 0 alloy shows a maximum isothermal magnetic entropy change (ASM) of 6.5 J/kg K under ambient pressure at RT, which is comparatively larger than that reported in many other Heusler systems at RT. Interestingly, ASM decreases with pressure for x = 0, while it shows an increasing trend for x = 2. A maximum refrigeration capacity of around 79 J/kg is observed for x = 0. Similar to the magnetic entropy change, the net magnetization for x = 0 and x = 2 show opposite trend under external pressure. This is explained by our ab initio simulation by closely inspecting the consequence of nonuniform strain along three crystallographic directions on the net magnetization. This actually arises due to considerable magnetocrystalline anisotropy in these alloys. The unconventional mechanism behind the influence of pressure on magnetic properties is also discussed in the light of varying bond lengths between different magnetic species, and hence on the antiferromagnetic/ferromagnetic exchange coupling strengths under pressure.

PHYSICAL REVIEW B 109[6], 064418, 2024. DOI: 10.1103/PhysRevB.109.064418

[P080-2024] "Measurement of the τ lepton polarization in Z boson decays in proton-proton collisions at √s=13 TeV"

Hayrapetyan, A.; Tumasyan, A.; Adam, W.; **Chinellato, J. A.***; et al.
CMS Collaboration

The polarization of tau leptons is measured using leptonic and hadronic tau lepton decays in Z -> tau(+)tau(-) events in proton-proton collisions at root s = 13 TeV recorded by CMS at the CERN LHC with an integrated luminosity of 36.3 fb(-1). The measured tau(-) lepton polarization at the Z boson mass pole is P-tau(Z) = -0.144 +/- 0.006 (stat) +/- 0.014 (syst) = -0.144 +/- 0.015, in good agreement with the measurement of the tau lepton asymmetry parameter of A(tau) = 0.1439 +/- 0.0043 = -P-tau(Z) at LEP. The tau lepton polarization depends on the ratio of the vector to axial-vector couplings of the tau leptons in the neutral current expression, and thus on the effective weak mixing angle sin(2)theta(eff)(W), independently of the Z boson production mechanism. The obtained value sin(2)theta(eff)(W) = 0.2319 +/- 0.0008(stat) +/- 0.0018(syst) = 0.2319 +/- 0.0019 is in good agreement with measurements at e(+)e(-) colliders.

JOURNAL OF HIGH ENERGY PHYSICS [1], 101, 2024. DOI: 10.1007/JHEP01(2024)101

[P081-2024] "Measurements of azimuthal anisotropy of nonprompt D0 mesons in PbPb collisions at √sNN=5.02 TeV"

Tumasyan, A.; Adam, W.; Andrejkovic, J. W.; **Chinellato, J. A.***; et al.
CMS Collaboration

Measurements of the elliptic (v(2)) and triangular (v(3)) azimuthal anisotropy coefficients are presented for D-0 mesons produced in b hadron decays (nonprompt D-0 mesons) in lead-lead collisions at root s(NN) = 5.02 TeV. The results are compared with previously published charm meson anisotropies measured using prompt D-0 mesons. The data were collected with the CMS detector in 2018 with an integrated luminosity of 0.58 nb(-1). Azimuthal anisotropy is sensitive to the interactions of quarks with the hot and dense medium created in heavy ion collisions. Comparing results for prompt and nonprompt D-0 mesons can assist in understanding the mass dependence of these interactions. The nonprompt results show lower magnitudes of v(2) and v(3) and weaker dependences on the meson transverse momentum and collision centrality than those found for prompt D-0 mesons. The results are in agreement with theoretical predictions that include a mass dependence in the interactions of quarks with the medium.

PHYSICS LETTERS B 850, 138389, 2024. DOI: 10.1016/j.physletb.2023.138389

[P082-2024] "Multi-Dirac and Weyl physics in heavy-fermion systems"

Silva, J. F.*; Miranda, E.*

We have studied multi-Dirac/Weyl systems with arbitrary topological charge n in the presence of a lattice of local magnetic moments. To do so we propose a multi-Dirac/Weyl Kondo lattice model which is analyzed through a mean-field approach appropriate to the paramagnetic phase. We study both the broken time-reversal and the broken inversion-symmetry Weyl cases. The multi-Dirac and broken time-reversal multi--Weyl cases have similar behavior, which is in contrast to the broken-parity case. For the former, low-energy particle-hole symmetry leads to the emergence of a critical coupling constant below which there is no Kondo quenching, reminiscent of the pseudogap Kondo impurity problem. Away from particle-hole symmetry, there is always Kondo quenching. For the broken inversion symmetry, there is no critical coupling.

Depending on the conduction electron filling, Kondo insulator, heavy-fermion metal, or semimetal phases can be realized. In the last two cases, quasiparticle renormalizations can differ widely between opposite chirality sectors, with characteristic dependences on microscopic parameters that could in principle be detected experimentally.

PHYSICAL REVIEW B 109[3], 035153, 2024. DOI: 10.1103/PhysRevB.109.035153

[P083-2024] "Multiplicity and event-scale dependent flow and jet fragmentation in pp collisions at √s=13 TeV and in p-Pb collisions at √sNN=5.02 TeV"

Acharya, S.; Adamova, D.; Rinella, G. A.; **Chinellato, D. D.*; Guardiano, G. G.*; Liveraro, G. S. S.*; Takahashi, J.***; et al.
ALICE Collaboration

Long- and short-range correlations for pairs of charged particles are studied via two-particle angular correlations in pp collisions at root s = 13TeV and p-Pb collisions at root s(NN) = 5.02TeV. The correlation functions are measured as a function of relative azimuthal angle Delta phi and pseudorapidity separation Delta eta for pairs of primary charged particles within the pseudorapidity interval vertical bar eta vertical bar < 0.9 and the transverse-momentum interval 1 < p(T) < 4 GeV/c. Flow coefficients are extracted for the long-range correlations (1.6 < vertical bar Delta eta vertical bar < 1.8) in various high-multiplicity event classes using the low-multiplicity template fit method. The method is used to subtract the enhanced yield of away-side jet fragments in high-multiplicity events. These results show decreasing flow signals toward lower multiplicity events. Furthermore, the flow coefficients for events with hard probes, such as jets or leading particles, do not exhibit any significant changes compared to those obtained from high-multiplicity events without any specific event selection criteria. The results are compared with hydrodynamic-model calculations, and it is found that a better understanding of the initial conditions is necessary to describe the results, particularly for low-multiplicity events.

JOURNAL OF HIGH ENERGY PHYSICS [3], 092, 2024. DOI: 10.1007/JHEP03(2024)092

[P084-2024] "Muon identification using multivariate techniques in the CMS experiment in proton-proton collisions at √s=13 TeV"

Hayrapetyan, A.; Tumasyan, A.; Adam, W.; **Chinellato, J. A.***; et al.
CMS Collaboration

The identification of prompt and isolated muons, as well as muons from heavy -flavour hadron decays, is an important task. We developed two multivariate techniques to provide highly efficient identification for muons with transverse momentum greater than 10 GeV. One provides a continuous variable as an alternative to a cut -based identification selection and offers a better discrimination power against misidentified muons. The other one selects prompt and isolated muons by using isolation requirements to reduce the contamination from nonprompt muons arising in heavy-flavour hadron decays. Both algorithms are developed using 59.7 fb-1 of proton-proton collisions data at a centre-of-mass energy of root s = 13 TeV collected in 2018 with the CMS experiment at the CERN LHC.

JOURNAL OF INSTRUMENTATION 19[2], P02031, 2024. DOI: 10.1088/1748-0221/19/02/P02031

[P085-2024] "New Structures in the J=ψJ=ψ Mass Spectrum in Proton-Proton Collisions at √ s=13 TeV"

Hayrapetyan, A.; Tumasyan, A.; **Chinellato, J. A.***; et al.
CMS Collaboration

A search is reported for near-threshold structures in the J=psi J=psi invariant mass spectrum produced in proton-proton collisions at ffiffi s p 1/4 13 TeV from data collected by the CMS experiment, corresponding to an integrated luminosity of 135 fb-1. Three structures are found, and a model with quantum interference among these structures provides a good description of the data. A new structure is observed with a local significance above 5 standard deviations at a mass of 6638 thorn 43 -38 ostat thorn thorn 16 -31 osyst thorn MeV. Another structure with even higher significance is found at a mass of 6847 thorn 44 -28 ostat thorn thorn 48 -20 osyst thorn MeV, which is consistent with the Xo6900 thorn resonance reported by the LHCb experiment and confirmed by the ATLAS experiment. Evidence for another new structure, with a local significance of 4.7 standard deviations, is found at a mass of 7134 thorn 48 -25 ostat thorn thorn 41 -15 osyst thorn MeV. Results are also reported for a model without interference, which does not fit the data as well and shows mass shifts up to 150 MeV relative to the model with interference

PHYSICAL REVIEW LETTERS 132[11], 111901, 2024. DOI: 10.1103/PhysRevLett.132.111901

[P086-2024] "Observation of WWγ Production and Search for Hγ Production in Proton-Proton Collisions at √ s=13 TeV"

Hayrapetyan, A.; Tumasyan, A.; Adam, W.; **Chinellato, J. A.***; et al.
CMS Collaboration

The observation of WW gamma production in proton -proton collisions at a center -of -mass energy of 13 TeV with an integrated luminosity of 138 fb-1 is presented. The observed (expected) significance is 5.6 (5.1) standard deviations. Events are selected by requiring exactly two leptons (one electron and one muon) of opposite charge, moderate missing transverse momentum, and a photon. The measured fiducial cross section for WW gamma is 5.9 +/- 0.8(stat) +/- 0.8(syst) +/- 0.7(modeling) fb, in agreement with the next -to -leading order quantum chromodynamics prediction. The analysis is extended with a search for the associated production of the Higgs boson and a photon, which is generated by a coupling of the Higgs boson to light quarks. The result is used to constrain the Higgs boson couplings to light quarks.

PHYSICAL REVIEW LETTERS 132[12], 121901, 2024. DOI: 10.1103/PhysRevLett.132.121901

[P087-2024] "On the Numerical Integration of the Multidimensional Kuramoto Model"

Aguiar, M. A. M. de*

The Kuramoto model, describing the synchronization dynamics of coupled oscillators, has been generalized in many ways over the past years. One recent extension of the model replaces the oscillators, originally characterized by a single phase, by particles with internal phases, represented by a point on the surface of the unit D-sphere. Particles are then more easily represented by D-dimensional unit vectors than by spherical angles. However, numerical integration of the state equations should ensure that the propagated vectors remain unit and that particles rotate on the sphere as predicted by the dynamical equations.As discussed in (Lee et al. in Journal of Statistical Mechanics: Theory and Experiment 2023(4):043403, 2023), integration of the three-dimensional Kuramoto model using Euler's method with time step not only changes the norm of the vectors but produces a small rotation of the particles around the wrong axis.

Importantly, the error in the axis' direction does not vanish in the limit. Therefore, instead of displacing the unit vectors in the direction of the velocity, one should perform a sequence of direct small rotations, as dictated by the equations of motion. This keeps the particles on the sphere at all times, ensuring exact norm preservation, and rotates the particles around the proper axis for small (Lee et al. in Journal of Statistical Mechanics: Theory and Experiment 2023(4):043403, 2023). Here, I propose an alternative way to do such integration by rotations in 3D that can be generalized to more dimensions using Cayley-Hamilton's theorem. Explicit formulas are provided for 2, 3, and 4 dimensions. I also compare the results with the fourth-order Runge–Kutta method, which seems to provide accurate results even requiring renormalization of the vectors after each integration step.

BRAZILIAN JOURNAL OF PHYSICS 54[4], 119, 2024. DOI: 10.1007/s13538-024-01493-z

[P088-2024] "Optimizing Josephson Junction Reproducibility in 30 kV E-Beam Lithography: An Analysis of Backscattered Electron Distribution"

Rebello, A. M.; **Ruela, L. M.*; Moreto, G.*;** Klein, N. Y.; Martins, E.; Oliveira, I. S.; Sinnecker, J. P.; **Rouxinol, F.***

This paper explores methods to enhance the reproducibility of Josephson junctions, which are crucial elements in superconducting quantum technologies, when employing the Dolan technique in 30 kV e-beam processes. The study explores the influence of dose distribution along the bridge area on reproducibility, addressing challenges related to fabrication sensitivity. Experimental methods include e-beam lithography, with electron trajectory simulations shedding light on the behavior of backscattered electrons. Wedescribe the fabrication of various Josephson junction geometries and analyze the correlation between the success rates of different lithography patterns and the simulated distribution of backscattered electrons. Our findings demonstrate a success rate of up to 96.3% for the double-resist 1-step low-energy e-beam lithography process. As a means of implementation strategy, we provide a geometric example that takes advantage of simulated stability regions to administer a controlled, uniform dose across the junction area, introducing novel features to overcome the difficulties associated with fabricating bridge-like structures.

NANOMATERIALS 14[9], 783, 2024. DOI: 10.3390/nano14090783

[P089-2024] "Order, chaos, and dimensionality transition in a system of swarmalators"

Lizárraga, J. U. F.*; O'Keeffe, K. P.; **Aguiar, M. A. M. de***

Similarly to sperm, where individuals self -organize in space while also striving for coherence in their tail swinging, several natural and engineered systems exhibit the emergence of swarming and synchronization. The arising and interplay of these phenomena have been captured by collectives of hypothetical particles named swarmalators, each possessing a position and a phase whose dynamics are affected reciprocally and also by the space -phase states of their neighbors. In this work, we introduce a solvable model of swarmalators able to move in two-dimensional spaces. We show that several static and active collective states can emerge and derive necessary conditions for each to show up as the model parameters are varied. These conditions elucidate, in some cases, the displaying of multistability among states.Notably, in the active regime, the system exhibits hyperchaos, maintaining spatial correlation under certain conditions and breaking it under others on what we interpret as a dimensionality transition.

PHYSICAL REVIEW E 109[4], 044209, 2024. DOI: 10.1103/PhysRevE.109.044209

[P090-2024] "Probing nuclear properties and neutrino physics with current and future CEvNS experiments"

Rossi, R. R.*; Garcia, G. S.; Tórtola, M.

The recent observation of coherent elastic neutrino-nucleus scattering (CEvNS) with neutrinos from pion decay at rest (N--DAR) sources by the COHERENT Collaboration has raised interest in this process in the search for new physics. Unfortunately, current uncertainties in the determination of nuclear parameters relevant to those processes can hide new physics effects. This is not the case for processes involving lower--energy neutrino sources such as nuclear reactors. Note, however, that a CEvNS measurement with reactor neutrinos depends largely on a (still-missing) precise determination of the quenching factor at very low energies, making its observation more challenging. In the upcoming years, once this signal is confirmed, a combined analysis of N-DAR and reactor CEvNS experiments will be very useful to probe particle and nuclear physics, with a reduced dependence on nuclear uncertainties. In this work, we explore this idea by simultaneously testing the sensitivity of current and future CEvNS experiments to neutrino nonstandard interactions (NSIs) and the neutron root mean square (rms) radius, considering different neutrino sources as well as several detection materials. We show how the interplay between future reactor and accelerator CEvNS experiments can help to get robust constraints on the neutron rms and to break degeneracies between the NSI parameters. Our forecast could be used as a guide to optimize the experimental sensitivity to the parameters under study.

PHYSICAL REVIEW D 109[9], 095044, 2024. DOI: 10.1103/PhysRevD.109.095044

[P091-2024] "Properties of AZO films grown by ALD applied as a TCO layer in perovskite solar cells"

Modesto, A. P. de. M. M.*; Merlo, R. B.*; Guzman, D. G.*; Barros, T. A. S.; Santos, T. E. A. dos; **Marques, F. C.***

In recent years, aluminum-doped zinc oxide (AZO) has attracted much attention due to its high transmittance and low resistivity, which makes it an excellent candidate for various applications in photovoltaic field, photoelectric, and transparent electronic devices. However, producing an AZO film with a desirable electronic property is still a challenge. In this work, we demonstrate that AZO can be successfully deposited by the atomic layer deposition (ALD) technique. The results showed that it is possible to dope ZnO with aluminum through the ALD technique using multiple layers composed of ZnO and Al2O3. Films with transmittance above 80%, optical band gap between 3.3 and 3.8 eV and promising electronic properties were obtained for use as a transparent conductive layer in large-area perovskite solar cells.

MRS ADVANCES, 2024. DOI: 10.1557/s43580-024-00873-6 Early Access Date: MAY 2024

[P092-2024] "Pseudorapidity dependence of anisotropic flow and its decorrelations using long-range multiparticle correlations in Pb-Pb and Xe-Xe collisions"

Acharya, S.; Adamova, D.; Adler, A.; **Chinellato, D. D.*; Guardiano, G. G.*; Jahnke, C.*; Liveraro, G. S. S.*; Takahashi, J.*;** et al.
ALICE Collaboration

The pseudorapidity dependence of elliptic (nu(2)), triangular (nu(3)), and quadrangular (nu(4)) flow coefficients of charged particles measured in Pb-Pb collisions at a centre-of-mass energy per nucleon pair of root s(NN) = 5.02 TeV and in Xe-Xe collisions at root s(NN) = 5.44 TeV with ALICE at the LHC are presented. The measurements are performed in the pseudorapidity range -3.5 < eta < 5 for various centrality intervals using two- and multi-particle cumulants with the subevent method. The flow probability density function (p.d.f.) is studied with the ratio of flow coefficient nu(2) calculated with four- and two-particle cumulant, and suggests that the variance of flow p.d.f. is independent of pseudorapidity. The decorrelation of the flow vector in the longitudinal direction is probed using two-particle correlations. The results measured with respect to different reference regions in pseudorapidity exhibit differences, argued to be a result of saturating decorrelation effect above a certain pseudorapidity separation, in contrast to previous publications which assign this observation to non--flow effects. The results are compared to 3 + 1 dimensional hydrodynamic and the AMPT transport model calculations. Neither of the models is able to simultaneously describe the pseudorapidity dependence of measurements of anisotropic flow and its fluctuations. The results presented in this work highlight shortcomings in our current understanding of initial conditions and subsequent system expansion in the longitudinal direction. Therefore, they provide input for its improvement.

PHYSICS LETTERS B 850, 138477, 2024. DOI: 10.1016/j.physletb.2024.138477

[P093-2024] "QCD challenges from pp to AA collisions: 4th edition"

Altmann, J.; Andres, C.; Andronic, A.; **Chinellato, D. D.***; et al.

This paper is a write-up of the ideas that were presented, developed and discussed at the fourth International Workshop on QCD Challenges from pp to AA, which took place in February 2023 in Padua, Italy. The goal of the workshop was to focus on some of the open questions in the field of high-energy heavy-ion physics and to stimulate the formulation of concrete suggestions for making progresses on both the experimental and theoretical sides. The paper gives a brief introduction to each topic and then summarizes the primary results.

EUROPEAN PHYSICAL JOURNAL C 84[4], 421, 2024. DOI: 10.1140/epjc/s10052-024-12650-8

[P094-2024] "Quantum approach to bound states in field theory"

Felipe, B. S.*; Pitelli, J. P. M.

It is well known that (possibly nonunique) suitable field dynamics can be prescribed in spacetimes with timelike boundaries by means of appropriate boundary conditions. In [R. M. Wald, J. Math. Phys. 21, 2802 (1980)], Wald derived a conserved energy functional for each prescribed dynamics. This conserved energy is related to the positive self-adjoint extensions of the spatial part A of the wave equation partial derivative 2 Phi/partial derivative t2 = -A Phi (A may not be, in principle, essentially self-adjoint). This is quite surprising since the canonical energy is not conserved in these cases. In this paper, we rederive this energy functional from an action principle (with appropriate boundary terms) following [A. A. Saharian, Phys. Rev. D 69, 085005 (2004)] and consider field dynamics arising from nonpositive self-adjoint extensions of A. The spectrum of the resulting theory fails to be positive and unstable mode solutions for classical fields come to light. By studying fields in halfMinkowski spacetime, we illustrate that these unstable classical solutions come as a consequence of an inverted parabolic potential governing their dynamics. From the quantum mechanical point of view, this leads to an effective inverted harmonic oscillator at the boundary. We then explore these unstable modes behavior, as well as their instabilities, at the quantum level.

PHYSICAL REVIEW D 109[10], 105013, 2024. DOI: 10.1103/PhysRevD.109.105013

[P095-2024] "Quantum biochemical analysis of the TtgR regulator and effectors"

Matias, E. G. de C.; Bezerra, K. S.; Costa, A. H. L.; Clemente Jr, W. S.; Oliveira, J. I. N.; Ribeiro Jr, L. A.; **Galvao, D. S.***; Fulco, U. L.

The recent expansion of multidrug-resistant (MDR) pathogens poses significant challenges in treating healthcare-associated infections. Although antibacterial resistance occurs by numerous mechanisms, active efflux of the drugs is a critical concern. A single species of efflux pump can produce a simultaneous resistance to several drugs. One of the best-studied efflux pumps is the TtgABC: a tripartite resistance-nodulation--division (RND) efflux pump implicated in the intrinsic antibiotic resistance in Pseudomonas putida DOT-T1E. The expression of the TtgABC gene is down-regulated by the HTH-type transcriptional repressor TtgR. In this context, by employing quantum chemistry methods based on the Density Functional Theory (DFT) within the Molecular Fragmentation with Conjugate Caps (MFCC) approach, we investigate the coupling profiles of the transcriptional regulator TtgR in complex with quercetin (QUE), a natural polyphenolic flavonoid, tetracycline (TAC), and chloramphenicol (CLM), two broad-spectrum antimicrobial agents. Our quantum biochemical computational results show the: [i] convergence radius, [ii] total binding energy, [iii] relevance (energetically) of the ligands regions, and [iv] most relevant amino acids residues of the TtgR-QUE/TAC/CLM complexes, pointing out distinctions and similarities among them. These findings improve the understanding of the binding mechanism of effectors and facilitate the development of new chemicals targeting TtgR, helping in the battle against the rise of resistance to antimicrobial drugs. These advances are crucial in the ongoing fight against rising antimicrobial drug resistance, providing hope for a future where healthcare-associated infections can be more beneficially treated.

SCIENTIFIC REPORTS 14[1], 8519, 2024. DOI: 10.1038/s41598-024-58441-9

[P096-2024] "Recent developments in agar-based optical devices"

Fujiwara, E.; Oku, H.; **Cordeiro, C. M. B.***

Biocompatible optical devices are breakthrough illumination, imaging, and biomedical sensing technologies. Despite the noteworthy developments in silk, cellulose, and hydrogel--based optics, such approaches rely on expensive precursors and intricate fabrication. Therefore, agar extracted from red algae emerges as a promising biodegradable alternative as an edible, low-cost, and renewable material. This paper overviews the state-of-the-art of agar-based optical devices. Firstly, we revisit this phycocolloid's fundamentals and highlight its appealing mechanical, optical, and electrical characteristics. Subsequently, we summarize the available agar elements, slab waveguides, and optical fibers. Lastly, we discuss their advantages and challenges by envisaging opportunities for future developments and applications.

MRS COMMUNICATIONS, 2024. DOI: 10.1557/s43579-024-00558-z, Early Access Date: MAY 2024

[P097-2024] "Search for Inelastic Dark Matter in Events with Two Displaced Muons and Missing Transverse Momentum in Proton-Proton Collisions at √s=13 TeV"

Hayrapetyan, A.; Tumasyan, A.; Adam, W.; **Chinellato, J. A.***; et al.
CMS Collaboration

A search for dark matter in events with a displaced nonresonant muon pair and missing transverse momentum is presented. The analysis is performed using an integrated luminosity of 138 fb-1 of protonproton (pp) collision data at a center -of -mass energy of 13 TeV produced by the LHC in 2016-2018. No significant excess over the predicted backgrounds is observed. Upper limits are set on the product of the inelastic dark matter production cross section sigma(pp -> A0 -> chi 1 chi 2) and the decay branching fraction B(chi 2 -> chi 1 mu thorn mu-), where A0 is a dark photon and chi 1 and chi 2 are states in the dark sector with near mass degeneracy. This is the first dedicated collider search for inelastic dark matter.

PHYSICAL REVIEW LETTERS 132[4], 041802, 2024. DOI: 10.1103/PhysRevLett.132.041802

[P098-2024] "Search for new Higgs bosons via same-sign top quark pair production in association with a jet in proton--proton collisions at √s=13 TeV"

Hayrapetyan, A.; Tumasyan, A.; Adam, W.; **Chinellato, J. A.***; et al,
CMS Collaboration

A search is presented for new Higgs bosons in proton-proton (pp) collision events in which a same-sign top quark pair is produced in association with a jet, via the pp -> tH/ A -> tt (c) over bar and pp -> tH/ A -> tt<(u)over bar processes. Here, H and A represent the extra scalar and pseudoscalar boson, respectively, of the second Higgs doublet in the generalized two-Higgs-doublet model (g2HDM). The search is based on pp collision data collected at a center-of-mass energy of 13 TeV with the CMS detector at the LHC, corresponding to an integrated luminosity of 138 fb(-1). Final states with a same-sign lepton pair in association with jets and missing transverse momentum are considered. New Higgs bosons in the 200-1000GeV mass range and new Yukawa couplings between 0.1 and 1.0 are targeted in the search, for scenarios in which either H or A appear alone, or in which they coexist and interfere. No significant excess above the standard model prediction is observed. Exclusion limits are derived in the context of the g2HDM.

PHYSICS LETTERS B 850, 138478, 2024. DOI: 10.1016/j.physletb.2024.138478

[P099-2024] "Search for Scalar Leptoquarks Produced via τ-Lepton-Quark Scattering in pp Collisions at ffiffi s p=13 TeV"

Hayrapetyan, A.; Tumasyan, A.; Adam, W.; **Chinellato, J. A.***; et al.
CMS Collaboration

The first search for scalar leptoquarks produced in z-lepton--quark collisions is presented. It is based on a set of proton--proton collision data recorded with the CMS detector at the LHC at a center-of-mass energy of 13 TeV corresponding to an integrated luminosity of 138 fb-1. The reconstructed final state consists of a jet, significant missing transverse momentum, and a z lepton reconstructed through its hadronic or leptonic decays. Limits are set on the product of the leptoquark production cross section and branching fraction and interpreted as exclusions in the plane of the leptoquark mass and the leptoquark-z-quark coupling strength.

PHYSICAL REVIEW LETTERS 132[6], 061801, 2024. DOI: 10.1103/PhysRevLett.132.061801

[P100-2024] "Skewness and kurtosis of mean transverse momentum fluctuations at the LHC energies"

Acharya, S.; Adamova, D.; Rinella, G. A.; **Chinellato, D. D.*; Guardiano, G. G.*; Liveraro, G. S. S.*; Takahashi, J.***; et al.
ALICE Collaboration

The first measurements of skewness and kurtosis of mean transverse momentum (< p(T)>) fluctuations are reported in Pb-Pb collisions at root s(NN) = 5.02 TeV, Xe-Xe collisions at root s(NN) = 5.44 TeV and pp collisions at root s = 5.02 TeV using the ALICE detector. The measurements are carried out as a function of system size < dN(ch)/d eta >(1/3)(vertical bar eta vertical bar<0.5), using charged particles with transverse momentum (p(T)) and pseudorapidity (eta), in the range 0.2 < p(T) < 3.0 GeV/c and vertical bar eta vertical bar < 0.8, respectively. In Pb-Pb and Xe-Xe collisions, positive skewness is observed in the fluctuations of < p(T)> for all centralities, which is significantly larger than what would be expected in the scenario of independent particle emission. This positive skewness is considered a crucial consequence of the hydrodynamic evolution of the hot and dense nuclear matter created in heavy-ion collisions. Furthermore, similar observations of positive skewness for minimum bias pp collisions are also reported here. Kurtosis of < p(T)> fluctuations is found to be in good agreement with the kurtosis of Gaussian distribution, for most central Pb-Pb collisions. Hydrodynamic model calculations with MUSIC using Monte Carlo Glauber initial conditions are able to explain the measurements of both skewness and kurtosis qualitatively from semicentral to central collisions in Pb-Pb system. Color reconnection mechanism in PYTHIA8 model seems to play a pivotal role in capturing the qualitative behavior of the same measurements in pp collisions.

PHYSICS LETTERS B 850, 138541, 2024. DOI: 10.1016/j.physletb.2024.138541

[P101-2024] "Spin Resistivity in a Metallic Channel Induced by Antiferromagnetic Approximation Effect"

Pimentel, D. P.*

This study presents experimental evidence of a potential alteration in the spin configuration of a conducting channel induced by the proximity effect of a highly frustrated antiferromagnetic insulator. Dicopper chloride trihydroxide Cu-2(OH)(3)Cl was employed as the highly frustrated antiferromagnetic insulator, while copper (Cu) served as the normal metal counterpart. Upon applying a voltage of 70 V to the sample volume, a copper conductive channel emerged within the antiferromagnetic insulator matrix. Literature reports indicate that Cu-2(OH)(3)Cl undergoes two magnetic transitions at T-N1 similar to 18 K and T-N2 similar to 6.4 K. Notably, an increase in resistance was experimentally observed precisely at the magnetic transition temperatures of Cu-2(OH)(3)Cl. This observation gains particular interest when considering the potential formation of a singlet state among the conductive channel spins influenced by the magnetism of Cu-2(OH)(3)Cl. Consequently, speculation arises that frustration might act as a "glue," facilitating the establishment of the singlet state within the conductive channel.

BRAZILIAN JOURNAL OF PHYSICS 54[3], 81, 2024. DOI: 10.1007/s13538-024-01443-9

[P102-2024] "Spin-state ordering and intermediate states in the mixed-valence cobalt oxyborate Co3O2BO3 with spin crossover"

Granado, E.*; Galdino, C. W.*; Moreno, B. D.; King, G.; Freitas, D. C.

Spin -state ordering-a periodic pattern of ions with different spin -state configurations along a crystal lattice-is a rare phenomenon, and its possible interrelation with other electronic degrees of freedom remains little explored. Here we perform a structural investigation of the mixed -valence Co homometallic ludwigite Co2+ 2 Co3+O2BO3. A superstructure consistent with a long-range Co3+ spin -state ordering is observed between T4 = 580 K and T3 = 510 K. Intermediate states with mesoscopic correlations are detected below T3 down to T1 = 480 K with a change of dimensionality at T2 = 495 K. The spin -state correlations are connected to the charge sector as revealed by the abrupt changes in the electrical resistance at T1 and T2. The evolution of the structural parameters below T1 indicate that the spin crossover is ignited by a moderate degree of thermally induced Co2+ and Co3+ charge disorder. Charge and spin -state degrees of freedom can be interrelated in mixed -valence spin -crossover materials, leading to sharp transitions involving intermediate spin -state and charge -correlated states at the mesoscale.

PHYSICAL REVIEW B 109[9], 094115, 2024. DOI: 10.1103/PhysRevB.109.094115

[P103-2024] "Strong Raman enhancement in structured colloids: localization of light"

Dipold, J.; Wetter, N. U.; **Marques, F. C.***; Freitas, A. Z.; Dogariu, A.; **Jiménez-Villar, E.***

Raman spectroscopy is a powerful technique for studying the interaction between light and matter. Here we show a significant enhancement of Raman emission over a broad range of pumping wavelengths from strongly scattering media comprising spatially correlated photonic structures of core-shell TiO 2 @Silica scatterers mixed with silica nanoparticles and suspended in ethanol. Long-range Coulomb interactions between nanoparticles inside these photonic colloidal structures induce a correlation in the scatterers' positions (TiO 2 @ Silica), affecting local and global photonic properties. The anomalous enhancement in Raman signal increases as the scattering strength is increased (through either scatterer concentration or pumping wavelength); however, the signal strength continues to behave linearly with excitation power, ruling out classical nonlinear and interferential phenomena. These observations may indicate strong photon correlation in strongly localized electromagnetic modes, inducing successive photon interactions with the atoms or molecules. Aside from the fundamental relevance to understanding measurable properties in this regime of strongly localized electromagnetic modes, our demonstration of strongly enhanced Raman emission over a broad range of pumping wavelengths provides new opportunities for the development of advanced photonic materials and devices. (c) 2024 Optica Publishing Group

JOURNAL OF THE OPTICAL SOCIETY OF AMERICA B-OPTICAL PHYSICS 41[6], 1415-1424, 2024. DOI: 10.1364/JOSAB.523100

[P104-2024] "Study of azimuthal anisotropy of γ(1S) mesons in pPb collisions at √SNN=8.16 TeV"

Tumasyan, A.; Adam, W.; **Chinellato, J. A.***; et al.
CMS Collaboration

The azimuthal anisotropy of gamma(1S) mesons in high-multiplicity proton-lead collisions is studied using data collected by the CMS experiment at a nucleon-nucleon center-of-mass energy of 8.16 TeV. The gamma(1S) mesons are reconstructed using their dimuon decay channel. The anisotropy is characterized by the second Fourier harmonic coefficients, found using a two-particle correlation technique, in which the gamma(1S) mesons are correlated with charged hadrons. A large pseudorapidity gap is used to suppress short-range correlations. Nonflow contamination from the dijet background is removed using a low-multiplicity subtraction method, and the results are presented as a function of gamma(1S) transverse momentum. The azimuthal anisotropies are smaller than those found for charmonia in proton-lead collisions at the same collision energy, but are consistent with values found for gamma(1S) mesons in lead-lead interactions at a nucleon-nucleon center-of-mass energy of 5.02 TeV.

PHYSICS LETTERS B 850, 138518, 2024. DOI: 10.1016/j.physletb.2024.138518

[P105-2024] "Synchrotron infrared nanospectroscopy in fourth-generation storage rings"

Santos, T. M.; **Lordano, S.*; Mayer, R. A.***; Volpe, L.; Rodrigues, G. M.; Meyer, B.; Westfahl Jr., H.; Freitas, R. O.

Fourth-generation synchrotron storage rings represent a significant milestone in synchrotron technology, offering outstandingly bright and tightly focused X-ray beams for a wide range of scientific applications. However, due to their inherently tight magnetic lattices, these storage rings have posed critical challenges for accessing lower-energy radiation, such as infrared (IR) and THz. Here the first-ever IR beamline to be installed and to operate at a fourth-generation synchrotron storage ring is introduced. This work encompasses several notable advancements, including a thorough examination of the new IR source at Sirius, a detailed description of the radiation extraction scheme, and the successful validation of our optical concept through both measurements and simulations. This optimal optical setup has enabled us to achieve an exceptionally wide frequency range for our nanospectroscopy experiments. Through the utilization of synchrotron IR nanospectroscopy on biological and hard matter samples, the practicality and effectiveness of this beamline has been successfully demonstrated. The advantages of fourth-generation synchrotron IR sources, which can now operate with unparalleled stability as a result of the stringent requirements for producing low-emittance X-rays, are emphasized.

JOURNAL OF SYNCHROTRON RADIATION 31, 547-556, 2024. DOI: 10.1107/S1600577524002364

[P106-2024] "Synthesis of lignin-based carbon/graphene oxide foam and its application as sensors for ammonia gas detection"

Rodrigues, J. S.; Freitas, A. D. M. de; Lima, L. F. de; Lopes, H. S. M.; Maciel, C. C.; Fré, L. V. B. V.; Pires, A. A. F.; Lima, V. H. de; Oliveira, V. J. R.; Olivati, C. de A.; Ferreira, M.; **Riul Jr., A***; Botaro, V. R.

The present study highlights the integration of lignin with graphene oxide (GO) and its reduced form (rGO) as a significant advancement within the bio-based products industry. Lignin -phenol -formaldehyde (LPF) resin is used as a carbon source in polyurethane foams, with the addition of 1 %, 2 %, and 4 % of GO and rGO to produce carbon structures thus producing carbon foams (CFs). Two conversion routes are assessed: (i) direct addition with rGO solution, and (ii) GO reduction by heat treatment. Carbon foams are characterized by thermal, structural, and morphological analysis, alongside an assessment of their electrochemical behavior. The thermal decomposition of samples with GO is like those having rGO, indicating the effective removal of oxygen groups in GO by carbonization. The addition of GO and rGO significantly improved the electrochemical properties of CF, with the GO2% sensors displaying 39 % and 62 % larger electroactive area than control and rGO2% sensors, respectively.

Furthermore, there is a significant electron transfer improvement in GO sensors, demonstrating a promising potential for ammonia detection. Detailed structural and performance analysis highlights the significant enhancement in electrochemical properties, paving the way for the development of advanced sensors for gas detection, particularly ammonia, with the prospective market demands for durable, simple, cost-effective, and efficient devices.

INTERNATIONAL JOURNAL OF BIOLOGICAL MACROMOLECULES 268, 131883, 2024. DOI: 10.1016/j.ijbiomac.2024.131883

[P107-2024] "The CYGNO experiment, a directional detector with optical readout for Dark Matter search"

Amaro, F. D.; Antonietti, R.; Baracchini, E.; **Kemp, E.***; et al.

The CYGNO experiment employs a gaseous Time Projection Chamber (TPC) in conjunction with Gas Electron Multipliers (GEMs) for amplification and optical readout. This configuration holds the potential to achieve precise 3D tracking down to O(1 keV) energies. The primary objective of this novel technique is to enable direct directional measurements of Dark Matter within our Galaxy. We assess the performance of the largest prototype, LIME, at Laboratori Nazionali del Gran Sasso (LNGS), including stability, energy response and resolution, using radioactive X-ray sources and Monte Carlo simulations. These findings will guide the fine-tuning of the CYGNO 04 demonstrator.

NUOVO CIMENTO C-COLLOQUIA AND COMMUNICATIONS IN PHYSICS 47[3], 126, 2024. DOI: 10.1393/ncc/i2024-24126-8

[P108-2024] "The infrared absorption spectrum of radioactive water isotopologue H215O"

Voronin, B. A.*; Tennyson, J.; Yurchenko, S. N.; Chesnokova, T. Y.; Chentsov, A. V.; Bykov, A. D.; Makarova, M. V.; Voronina, S. S.; **Cruz, F. C.***

A room temperature line list for the H215O radioactive isotopologue of the water molecule is computed using the variational nuclear-motion DVR3D program suite and an empirical high-precision potential energy function. The line list consists of rotation-vibrational energies and Einstein -A coefficients, covering a wide spectral range from 0 to 25000 cm-1 and the total angular momenta J up to 30. Estimates of air-broadening coefficients are provided. Experimentally derived energies of H216O, H217O and H218O from the literature are used to provide improved energies for important states with uncertainty estimates for the H215O. A number of the wmost promising spectroscopic ranges for the detection of H215O are proposed. The calculated absorption spectrum should be useful for the study gaseous radioactive water at IR region, determining concentration, etc.

SPECTROCHIMICA ACTA PART A-MOLECULAR AND BIOMOLECULAR SPECTROSCOPY 311, 124007, 2024. DOI: 10.1016/j.saa.2024.124007

[P109-2024] "Thermal Hall conductivity of a valence bond solid phase in the square lattice J1-J2 antiferromagnet Heisenberg model with a Dzyaloshinskii-Moriya interaction"

Buzo, L. S.*; Doretto, R. L.*

We calculate the thermal Hall conductivity kappa xy for the columnar valence bond solid phase of a two-dimensional frustrated antiferromagnet. In particular, we consider the square lattice spin-1/2 J1-J2 antiferromagnetic Heisenberg model with an additional Dzyaloshinskii-Moriya interaction between the spins and in the presence of an external magnetic field. We concentrate on the intermediate parameter region of the J1-J2 model, where a quantum paramagnetic phase is stable, and consider a Dzyaloshinskii-Moriya vector pattern associated with the couplings between the spins in the CuO2 planes of the YBa2Cu3O6 compound. We describe the columnar valence bond solid phase within the bond-operator formalism, which allows us to map the Heisenberg model into an effective interacting boson model written in terms of triplet operators. The effective boson model is studied within the harmonic approximation, and the triplon excitation bands of the columnar valence bond solid phase are determined. We then calculate the Berry curvature and the Chern numbers of the triplon excitation bands and, finally, determine the thermal Hall conductivity due to triplons as a function of the temperature. We find that the Dzyaloshinskii-Moriya interaction yields a finite Berry curvature for the triplon bands, but the corresponding Chern numbers vanish. Although the triplon excitations are topologically trivial, the thermal Hall conductivity of the columnar valence bond solid phase in the square lattice antiferromagnet is finite at low temperatures. Our results complement a previous study by Samajdar et al., Phys. Rev. B 99, 165126 (2019) concerning the thermal Hall effect due to spinons of a spin-liquid phase on a square lattice. We also comment on the relations of our results with a no-go condition for a thermal Hall effect previously derived for ordered magnets by Katsura et al.,

PHYSICAL REVIEW B 109[13], 134405, 2024. DOI: 10.1103/PhysRevB.109.134405

[P110-2024] "Thickness dependent tribological and magnetic behavior of two-dimensional cobalt telluride (CoTe2)"

Slathia, S.; Wei, C. C.; Tripathi, M.; **Tromer, R.***; Negedu, S. D.; Boland, C. S.; Sarkar, S.; **Galvao, D. S.***; Dalton, A.; Tiwary, C. S.

Two-dimensional (2D) layered transition-metal based tellurides (chalcogens) are known to harness their surface atoms' characteristics to enhance topographical activities for energy conversion, storage, and magnetic applications. The gradual stacking of each sheet alters the surface atoms' subtle features such as lattice expansion, leading to several phenomena and rendering tunable properties. Here, we have evaluated thickness-dependent mechanical properties (nanoscale mechanics, tribology, potential surface distributions, interfacial interaction) of 2D CoTe2 sheets and magnetic behavior using surface probe techniques. The experimental observations are further supported and explained with theoretical investigations: density functional theory and molecular dynamics. The variation in properties observed in theoretical investigations unleashes the crucial role of crystal planes of the CoTe2. The presented results are beneficial in expanding the use of the 2D telluride family in flexible electronics, piezo sensors, tribo-generators, and next-generation memory devices.

2D MATERIALS 11[3], 035006, 2024. DOI: 10.1088/2053-1583/ad3cec

[P111-2024] "Two-particle Bose-Einstein correlations and their Lévy parameters in PbPb collisions at √sNN=5.02 TeV"

Tumasyan, A.; Adam, W.; Andrejkovic, J. W.; **Chinellato, J. A.***; et al.
CMS Collaboration

Two -particle Bose-Einstein momentum correlation functions are studied for charged-hadron pairs in lead -lead collisions at a center -of -mass energy per nucleon pair of .'/ sNN = 5.02 TeV. The data sample, containing 4.27 x 109 minimum bias events corresponding to an integrated luminosity of 0.607 nb-1, was collected by the CMS experiment in 2018.

The experimental results are discussed in terms of a Levy--type source distribution. The parameters of this distribution are extracted as functions of particle pair average transverse mass and collision centrality. These parameters include the Levy index or shape parameter alpha, the Levy scale parameter R, and the correlation strength parameter lambda. The source shape, characterized by alpha, is found to be neither Cauchy nor Gaussian, implying the need for a full Levy analysis. Similarly to what was previously found for systems characterized by Gaussian source radii, a hydrodynamical scaling is observed for the Levy R parameter. The lambda parameter is studied in terms of the core -halo model.

PHYSICAL REVIEW C 109[2], 024914, 2024. DOI: 10.1103/PhysRevC.109.024914

[P112-20224] "Typical values statistical analysis for adult chest and abdomen-pelvis CT examinations"

Costa, P. R.; Castro, J. C. de O.; Nunes, I. P. F.; Nersissian, D. Y.; Sawamura, M. Y.; Leao, H.; **Tomal, A.***

The use of DRLs has been extensively documented in the literature as a tool for protocol optimization across different x-ray imaging modalities in different countries. It recognizes the importance of developing and validating methods capable of correlating DRL quantities (CTDIvol, DLP and SSDE) with the technical parameters employed in CT studies. Such correlations must be supported by robust statistical methodologies in order to ensure the adoption of adequate optimization decisions. The aim of this work was to apply the Generalized Additive Model (GAM) statistical analysis in adult non-contrast chest and abdomen-pelvis CT typical values. These patient cohorts were statistically evaluated to identify correlations with key-parameters associated to the demographic patient information and machine dependent data, taking into account patients' effective diameters, d, and body mass indexes (BMI). GAM was implemented considering each anatomical region in order to correlate the log-transformed DRL quantities (DRLq's) as outcomes given different key predictors related to image acquisition and patient characteristics. A total of 956 CT patient data were collected in this retrospective singlecenter study. Demographic variables demonstrate that age is not or it is just weakly-correlated to the DRLq's resulting from chest procedures, but it is strongly correlated when considering abdomen-pelvis examinations. Gender is correlated to the DRLq's for chest examinations adopting d as a key predictor but it is only correlated with DLP adopting the BMI as a key predictor. The level of accuracy provided by the GAM was adequate for interpreting the large fluctuations of the DRLq's, technical parameters and demographic data observed for the studied patient cohorts. Our results reflect the importance of a comprehensive statistical evaluation of typical values. The domain of this technique is important to different CT imaging chain stakeholders and its application can be a key tool for decision-making process to effective optimization strategies.

RADIATION PHYSICS AND CHEMISTRY 221, 111669, 2024. DOI: 10.1016/j.radphyschem.2024.111669

[P113-2024] "Xenon Nanobubbles and Residual Defects in Annealed Xe-Implanted Si(001): Analysis by the Combination of Advanced Synchrotron X-Ray Diffraction and Transmission Electron Microscopy Techniques"

Calligaris, G. A.; Lang, R.; Bettini, J.; Santos, A. O. dos; **Cardoso, L. P.***

Residual crystalline defects on the subsurface of Xe-implanted Si(001) and post-annealed substrates are investigated by advanced X-ray diffraction and transmission electron microscopy techniques. Local characterization highlights the features of recrystallization and structural evolution induced by thermal treatments resulting from the formation of gaseous Xe nanobubbles embedded in a heavily twinned surrounding Si matrix. Both mappings of conventional reciprocal space and X-ray multiple-beam diffraction exhibited different aspects from the kinematical and dynamical X-ray theories, respectively, contributing to a better understanding and description approach of residual damage in ion-beam implanted materials. A simple layered model is proposed based on the experimental Q-Scans profiles and computational calculations, distinguishing host matrix structural strain artifacts from the Xe-bubbles pressure probed by a Xe M4,5-edge blue shift in EELS spectra. Bubble pressure is determined by extrapolating the equation of state for xenon at high temperatures. The study also supports an experimental constant CXeM-edge for the increment E approximately equal to C n theoretical expression. Xe-nanobubbles formation, residual damages in Xe+-implanted Si substrate, and its evolution under thermal annealing are investigated in this study. Advanced X-ray diffraction and transmission electron microscopy techniques reveal different aspects of Si recrystallization in the presence of xenon. A layered model is proposed based on the experimental data and calculations, distinguishing Si matrix structural strain artifacts from the pressurized bubbles.

ADVANCED MATERIALS TECHNOLOGIES, 2024. DOI: 10.1002/admt.202301621 Early Access Date: APR 2024

[P114-2024] "ψ(2S) Suppression in Pb-Pb Collisions at the LHC"

Acharya, S.; Adamova, D.; Adler, A.; **Chinellato, D. D.*; Guardiano, G. G.*; Jahnke, C.*; Takahashi, J.***; et al.
ALICE Collaboration

The production of the psi(2S) charmonium state was measured with ALICE in Pb-Pb collisions at root s(NN) = 5.02 TeV, in the dimuon decay channel. A significant signal was observed for the first time at LHC energies down to zero transverse momentum, at forward rapidity (2.5 < y < 4). The measurement of the ratio of the inclusive production cross sections of the psi(2S) and J/psi resonances is reported as a function of the centrality of the collisions and of transverse momentum, in the region p(T) < 12 GeV/c. The results are compared with the corresponding measurements in pp collisions, by forming the double ratio [sigma(psi(2S)) /sigma(J/psi)](Pb-Pb)/[sigma(psi(2S)) / sigma(J/psi)](pp). It is found that in Pb-Pb collisions the psi(2S) is suppressed by a factor of similar to 2 with respect to the J/psi. The psi(2S) nuclear modification factor R-AA was also obtained as a function of both centrality and p(T). The results show that the psi(2S) resonance yield is strongly suppressed in Pb-Pb collisions, by a factor of up to similar to 3 with respect to pp. Comparisons of cross section ratios with previous Super Proton Synchrotron findings by the NA50 experiment and of R-AA with higher-p(T) results at LHC energy are also reported. These results and the corresponding comparisons with calculations of transport and statistical models address questions on the presence and properties of charmonium states in the quark-gluon plasma formed in nuclear collisions at the LHC.

PHYSICAL REVIEW LETTERS 132[4], 042301, 2024. DOI: 10.1103/PhysRevLett.132.042301

***Autores da comunidade IFGW**
Fonte: Web of Science on-line (WOS)

Eventos publicados

[P115-2024] "Post-2000 progress in nonlinear optics: tabulating new materials and best practices"

Vermeulen, N.; Espinosa, D.; Ball, A.; **Padilha Junior, L. A.***; et al.
Schunemann P. G. (Ed.)

The field of nonlinear optics (NLO), launched about 60 years ago, has gained considerable momentum over the past two decades, resulting in an enormous growth in NLO publications for a wide range of material categories, including bulk materials, 0D-1D-2D materials, metamaterials, fiber waveguiding materials, on-chip waveguiding materials, and hybrid waveguiding systems. However, a convenient summary of NLO data collected since 2000 for these different material types has been lacking and would be a valuable resource for researchers in the field. Here, we present a new set of data tables showcasing a representative list of NLO properties taken from the literature since 2000 on the above-mentioned material categories. Furthermore, we provide best practices for performing and reporting NLO experiments. These best practices underpin the selection process that we used for including papers in the tables, and also form the foundation for a more adequate comparison, interpretation, and use of the NLO parameters published today and those that will be published in the future.

NONLINEAR FREQUENCY GENERATION AND CONVERSION: MATERIALS AND DEVICES XXIII, Book Series: Proceedings of SPIE, Volume: 12869 Article Number: 128690D, 2024. DOI: 10.1117/12.3003245

Cartas publicadas

[Ca001-2024] "Extracellular matrix in leg basal cell carcinoma: Possible pathogenetic role of chronic venous insufficiency"

Sala, A. C. A.; Ueda, P. H. H.; Buffo, T. H.; Velho, P. E. N. F.; **Pelegati, V. B.*; Cesar, C. L.*;** Cintra, M. L.; Vieira-Damiani, G.; Amstalden, E. M. I.

SKIN RESEARCH AND TECHNOLOGY 30[6], e13805, 2024. DOI: 10.1111/srt.13805

***Autores da comunidade IFGW**
Fonte: Web of Science on-line (WOS)

Defesas de Dissertações do IFGW

[D011-2024] "Interferômetros Programáveis para Testes de Contextualidade e Não-Localidade em Sistemas Quânticos"
Aluno: Luiz Henrique Peres Siqueira
Orientador: Prof. Dr. Pierre Louis de Assis
Data: 27/05/2024

[D012-2024] "Investigação de Redes Hiperbólicas Planares Usando Circuitos Supercondutores"
Aluno: Ednilson dos Santos Lopes da Cunha
Orientador: Prof. Dr. Francisco Paulo Marques Rouxinol
Data: 05/06/2024

[D013-2024] "Hanbury Brown-Twiss effect for inflationary cosmology"
Aluno: Gustavo Matheus Gauy
Orientador: Prof. Dr. Donato Giorgio Torrieri
Data: 14/06/2024

[D014-2024] "Estudo por Espalhamento Raman do Iridato Sr IrO com substituições isovalentes de Ca 2 4 e Ba no sítio do Sr"
Aluno: Adimir Italo Vilca Morales
Orientador: Prof. Dr. Eduardo Granado Monteiro da Silva
Data: 26/06/2024

[D015-2024] "Formação e caracterização de compósitos flexíveis para desenvolvimento de sensores tácteis"
Aluno: Patrícia Duarte de Almeida
Orientador: Profa. Dra. Mônica Alonso Cotta
Data: 03/07/2024

Defesas de Teses do IFGW

[T007-2024] "Sondando graus de liberdade eletrônicos, magnéticos e estruturais de novos materiais utilizando técnicas de difração e espectroscopia"
Aluno: Rodolfo Tartaglia Souza
Orientador: Prof. Dr. Eduardo Granado Monteiro da Silva
Data: 17/05/2024

[T008-2024] "Estudos de dispositivos de ondas acústicas de superfície e fotoluminescência de nanofios semicondutores"
Aluno: João Vítor Chiaramonte Rocha
Orientador: Prof. Dr. Francisco Paulo Marques Rouxinol
Data: 27/05/2024

[T009-2024] "Obtenção das Propriedades Ópticas e Dinâmicas do Tecido Biológico com Técnicas de Espectroscopia Óptica de Difusão"
Aluno: Giovani Grisotti Martins
Orientador: Prof. Dr. Rickson Coelho Mesquita
Data: 06/06/2024

[T010-2024] "Integrated Brillouin-optomechanics in Low--losses Materials"
Aluno: Roberto de Oliveira Zurita
Orientador: Prof. Dr. Thiago Mayer Alegre
Data: 07/06/2024

Fonte: Portal IFGW/Eventos
Disponível em: https://portal.ifi.unicamp.br/a-instituicao/eventos/month.calendar/2023/12/14/-

Defesas de Dissertações e Teses do PECIM

[P003-2024] "Grupo de estudos de tendência reflexiva e colaborativa e o desenvolvimento profissional de professoras e professores que ensinam ciências"
Aluno: Daniel Fernando Matsuzaki da Silva
Orientador: Prof. Dr. Jorge Megid Neto
Banca: PProf. Dr. Jorge Megid Neto - orientador, Prof. Dr. Mauricio Compiani - IG/ UNICAMP, Dr. Leonir Lorenzetti - Departamento de Química - Universidade Federal do Paraná /Curitiba, Dra. Eliete Aparecida de Godoy - Pontifícia Universidade Católica de Campinas /Campinas, **Dr. Fernando Jorge da Paixão Filho- IFGW / Unicamp /Campinas**, Profa Dra Alessandra Aparecida Viveiro - FE/Unicamp (Suplente), Profa. Dra. Juliana Rink - FE/ UNICAMP (Suplente), Dr. Paulo Marcelo Marini Teixeira - Universidade Estadual do Sudoeste da Bahia /Vitória da Conquista, Dra. Jussara Cristina Barboza Tortella - Pontifícia Universidade Católica de Campinas / Campinas
Data: 14/06/2024
Exame de Defesa: Doutorado

[P004-2024] "Insucesso em cálculo I: um estudo de caso no campus da UFERSA em Pau Dos Ferros-Rn"
Aluno: Monica Paula de Sousa Martins
Orientador: Prof. Dr. Lucio Tunes dos Santos
Banca: Prof. Dr. Lucio Tunes dos Santos - orientador, Profa. Dra. Laura Leticia Ramos Rifo - IMECC/Unicamp, **Prof. Dr. Mauricio Urban Kleinke - IFGW/Unicamp,** Prof. Dr. Samuel Rocha de Oliveira - IMECC/Unicamp - suplente, Profa. Dra. Rita Santos Guimarães - IMECC/Unicamp - suplente
Data: 27/05/2024
Exame de Defesa: Doutorado

[P005-2024] "Percepções de alguns formadores sobre ações entre 2012 a 2021: o olhar dos formadores sobre os processos formativos da Diretoria de Ensino Campinas Oeste"
Aluno: Paulo Rogério da Silva
Orientador: Prof. Dr. Gildo Girotto Júnior
Banca: Profa. Dra. Ana de Medeiros Arnt (Presidente) Instituição de Origem: IB/ UNICAMP, Profa. Dra. Ivana Elena Camejo Aviles Instituição de Origem: IB/ UNICAMP , **Prof. Dr. Guilherme Stecca Marcom Instituição de Origem: IFGW/ UNICAMP**, Dra. Lilian Patrícia Lima Instituição de Origem: Universidade Federal de Lavras /Lavras, Dr. Joao Batista dos Santos Junior Instituição de Origem: UFSCAR /Araras, Prof. Dr. Leandro Antonio de Oliveira Instituição de Origem: IQ/ UNICAMP - suplente, Dra. Luciane Fernandes de Goes Instituição de Origem: Centro Estadual de Educação Tecnológica Paula Souza /Campinas - suplente, Profa. Dra. Dora Maria Grassi Kassisse Instituição de Origem: IB/ UNICAMP - suplente, Dr. Ivo Bernardi de Freitas - Pesquisador Independente / Campinas - suplente
Data: 24/05/2024
Exame de Defesa: Doutorado

Fonte: Página do PECIM
Disponível em: https://www.pecim.unicamp.br/bancas

Abstracta

Instituto de Física
Diretor: Profa. Dra. Mônica Alonso Cotta
Diretora Associada: Prof. Dr. Marcos Cesar de Oliveira
Universidade Estadual de Campinas - UNICAMP
Cidade Universitária Zeferino Vaz
13083-859 - Campinas - SP - Brasil
e-mail: secdir@ifi.unicamp.br
Fone: +55 19 3521-5300

Publicação

Biblioteca do Instituto de Física Gleb Wataghin
http://portal.ifi.unicamp.br/biblioteca
Instagram: @bif.unicamp

Diretora Técnica: Sandra Maria Carlos Cartaxo
Coordenadora da Comissão de Biblioteca: Profa. Dra. Arlene Cristina Aguilar

Elaboração e editoração:
Maria Graciele Trevisan (Bibliotecária)
Artes gráficas: Júlia da Silva Oliveira (Estagiária)
Contato: infobif@ifi.unicamp.br